ACS OMEGA

http://pubs.acs.org/journal/acsodf

Article

Stabilizing Triglyceride in Methanol Emulsions via a Magnetic Pickering Interfacial Catalyst for Efficient Transesterification under Static Conditions

Hao Zhang, Siyang Yu, Shixiong Cao, Xiaobo Liu, Jun Tang, Lingyu Zhu, Jianbing Ji, and Jianli Wang*

Cite This: *ACS Omega* 2021, 6, 14138−14147

Read Online

ACCESS | Metrics & More | Article Recommendations | Supporting Information

ABSTRACT: Pickering emulsion systems provide potential platforms for simultaneously intensifying and catalyzing transesterification between triglyceride and methanol under static conditions. However, realizing static transesterification with high biodiesel yield is still challenging due to low emulsion stability at the reaction temperature. Here, a series of magnetically recyclable Pickering interfacial catalysts (PICs) with similar surface affinities but different densities were constructed as stabilizers of a soybean oil/methanol emulsion. The variations in the emulsion volume fraction and droplet size were comparatively studied and analyzed from the viewpoint of droplet settling and catalyst particle shedding. It is found that, except for surface affinity, PIC density also plays a pivotal role in emulsion stability owing to the non-negligible effect of gravity on catalyst adsorption in triglyceride/methanol emulsion (especially at elevated temperature). By reducing the density, finely improving the lipophilicity, and optimizing the addition amount of PIC, the obtained soybean oil/methanol emulsion can remain stable for at least 12 h at 60 °C, enabling static transesterification with a high biodiesel yield of 95.6%. Moreover, the best performing PIC can be reused for at least 7 cycles. This efficient static transesterification system offers a green strategy for biodiesel production.

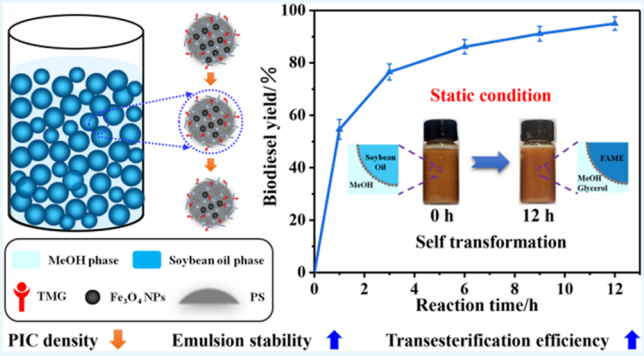

1. INTRODUCTION

Biodiesel, as a clean and renewable biofuel, has aroused growing interest among research communities due to the depletion of fossil fuels and serious environmental pollution.[1−3] In industry, biodiesel is commonly produced by catalytic transesterification of triglyceride with methanol,[4,5] yielding long-chained fatty acid methyl esters (FAME).[6,7] The immiscible triglyceride and methanol constitutes a liquid−liquid biphasic system, which always encounters the issue of low reaction efficiency due to high mass transfer resistance.[8] To accelerate the transesterification rate, various intensification methods such as stirring,[9] ultrasonic[10] and microwave treatment,[11] and hydrodynamic cavitation[12,13] were applied to strongly mix the two phases, thus enlarging the interfacial area for more efficient reactant contact. These methods rely on continuous energy input to balance out the cohesive energy of dispersed droplets. However, most of the input energy is eventually dissipated as internal energy due to low energy transmission and conversion efficiency, resulting in significant energy waste.

In recent years, Pickering emulsion (emulsion stabilized by solid particles) has been developed as a versatile platform for overcoming mass transfer obstacles of liquid−liquid biphasic reactions.[14−17] The solid particles in a Pickering emulsion can simultaneously act as an emulsion stabilizer and a catalyst,[18,19] namely Pickering interfacial catalyst (PIC).[14,20] In a Pickering emulsion, the highly dispersed droplets not only lead to a large interfacial contact area but also prominently shortened diffusion distance between reactant molecules.[21,22] Hence, a stable Pickering emulsion makes it possible to realize a high reaction rate without continuous stirring (static condition),[23−25] which is beneficial for reducing energy consumption. For instance, Yang et al. found that the reaction efficiency of lipase-catalyzed hydrolytic kinetic resolution of racemic esters in the static Pickering emulsion system is comparable to that of the conventional stirrer-driven biphasic systems.[26] Wang et al. employed amphiphilic carbon−organosilica Janus particles containing phosphotungstic active component as PICs to stabilize an *n*-octane/acetonitrile emulsion for fuel oil desulfurization, and a high desulfurization ratio was obtained without stirring.[27] According to the

Received: February 3, 2021
Accepted: May 13, 2021
Published: May 24, 2021

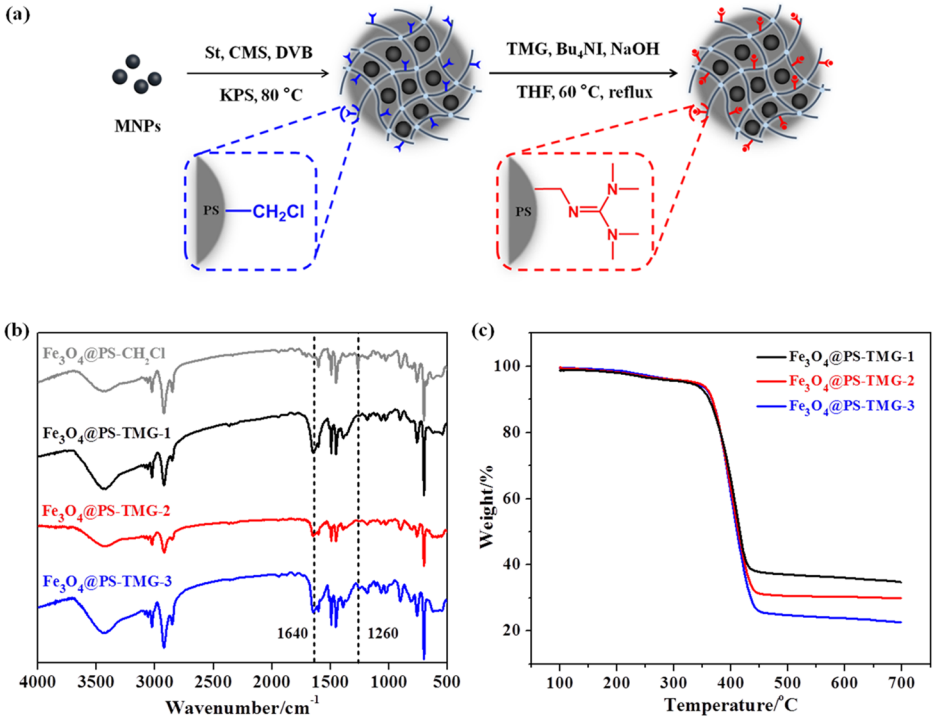

Figure 1. (a) Schematic diagram of the preparation of the nanocatalysts. (b) Fourier transform infrared (FTIR) spectra of Fe_3O_4@PS-CH_2Cl and Fe_3O_4@PS-TMG-*n* (*n* = 1−3). (c) Thermogravimetry (TG) curves of Fe_3O_4@PS-TMG-*n* (*n* = 1−3).

literature,[28,29] the surface affinity of PIC plays a dominant role in emulsion stability (a critical factor for realizing an efficient static reaction). In our previous work, we have developed a series of magnetic PICs loaded with tetramethylpiperidinooxy.[30−32] The magnetic PICs with optimized hydrophobicity can not only be used to stabilize the water/dichloromethane emulsion for selective oxidation of alcohols under static conditions but can also be conveniently recovered using a magnet.[32]

Considering the merits of high performance and easy recovery of magnetic PICs, recently, we constructed several magnetic PICs loaded with organic base 1,1,3,3-tetramethylguanidine (TMG) for catalyzing transesterification of soybean oil (triglyceride) with methanol,[33] and realized a high biodiesel yield (98.6%) under low-speed stirring (300 rpm). The use of a magnetic recyclable PIC also simplifies the biodiesel production process and reduces the generation of waste pollutants, which overcomes the drawbacks of the most widely adopted alkaline catalyst (KOH) in industry.[34,35] However, merely adjusting the surface affinity of the magnetic PICs failed to make the static soybean oil/methanol emulsions remain stable for enough time at the reaction temperature. Under static conditions, the ex-field that causes emulsion destabilization must be gravity.[36,37] In aqueous−organic type emulsion, the gravity of PICs is normally ignored due to their small size, and the adsorption of PICs at water−oil interface is extremely stable owing to large interfacial tension.[38] We note that the soybean oil/methanol emulsion is an organic−organic biphasic system, which presents much smaller interfacial tension than that of aqueous−organic systems.[39] Therefore, the adsorption of the magnetic PICs at the soybean oil−methanol interface is expected to be less stable than that of aqueous−organic systems. Under this circumstance, gravity might have a significant influence on emulsion stability. As is well known, the force of gravity on an object is closely related to its density. To construct a more stable platform for realizing efficient transesterification under static conditions, it is necessary to modulate the density of the magnetic PICs and further explore the underlying stability mechanism of the triglyceride/methanol biphasic emulsion system. To the best of our knowledge, the effect of PIC density on emulsion stability has rarely been reported.

Herein, we first designed and synthesized a series of magnetic PICs with a similar TMG loading amount but different densities based on the Fe_3O_4 core and polystyrene (PS) shell, and systematically investigated their performance on the stabilization of a soybean oil/methanol emulsion. The variations in the emulsion volume fraction and droplet size were analyzed from the viewpoint of droplet settling and catalyst particle shedding. The experimental results and force analysis revealed that, except for optimizing surface affinity, adjusting the density of PIC particles is also critical to realizing a long-time stable triglyceride/methanol emulsion. Then, by keeping the density of PIC close to that of the continuous phase, finely improving the lipophilicity, and optimizing the addition amount of PIC particles, the obtained soybean oil/methanol emulsion remains stable for at least 12 h at 60 °C, which enables self-transformation of triglyceride to FAME under static conditions with a high yield of 95.6%. Furthermore, the best performing catalyst can be quickly recovered with a magnet and reused for at least 7 cycles.

2. EXPERIMENTAL SECTION

2.1. Materials and Reagents. $FeCl_3·6H_2O$ (≥99%), $FeSO_4·7H_2O$ (≥99%), ammonia solution ($NH_3·H_2O$, 25−28%), oleic acid (OA, ≥93%), octane (≥99%), styrene (St, 99%), 4-chloromethyl styrene (CMS, ≥90%), divinylbenzene (DVB, 80%), *n*-hexadecane (98%), sodium dodecyl sulfate (SDS, ≥99%), potassium persulfate (KPS, ≥99%), 1,1,3,3-tetramethylguanidine (TMG, 99%), Bu_4NI (≥99%), tetrahy-

https://doi.org/10.1021/acsomega.1c00629
ACS Omega 2021, 6, 14138−14147

Table 1. Experimental Conditions and Characterization Results of Fe_3O_4@PS-TMG-n (n = 1−5)

sample	Fe_3O_4 concentration (wt %)	n_{St}:n_{CMS}	TMG loading (mmol/g)	$\rho_{particle}$ (kg/m^3)	methanol CA (deg)	soybean oil CA (deg)
Fe_3O_4@PS-TMG-1	46	3:1	0.488	1413.3	9 ± 2	30 ± 2
Fe_3O_4@PS-TMG-2	38	3:1	0.495	1306.2	8 ± 1	31 ± 2
Fe_3O_4@PS-TMG-3	30	3:1	0.506	1069.1	8 ± 2	30 ± 1
Fe_3O_4@PS-TMG-4	30	3.15:1	0.498	1045.8	11 ± 1	27 ± 1
Fe_3O_4@PS-TMG-5	30	3.3:1	0.491	1040.2	14 ± 1	23 ± 1

drofuran (THF, 99.0%), NaOH (97%), anhydrous sodium sulfate (99%), and methanol were purchased from Aladdin Co. Ltd. Refined soybean oil (molecular weight of 882 g/mol, acid value of 0.12 mg KOH/g) was obtained from Zhejiang Yihai Kerry Food Industry Co., Ltd.

2.2. Preparation of Magnetic Nanocatalysts Loaded with TMG. The magnetic nanocatalysts were prepared according to the previously reported procedure shown in Figure 1a.[33] First, the magnetic nanoparticles (MNPs) consisting of oleic acid functionalized Fe_3O_4 was dispersed in octane to get a ferrofluid. Then, a certain amount of styrene, 4-chloromethyl styrene, and divinylbenzene were added to the ferrofluid, which would be added into aqueous solution containing SDS. After emulsification, KPS was added and the mixture was heated to 80 °C for 17 h to obtain magnetic nanospheres Fe_3O_4@PS-CH_2Cl. Afterward, Fe_3O_4@PS-CH_2Cl, TMG, Bu_4NI, NaOH, H_2O, and THF were placed in a reactor and the mixture was refluxed at 60 °C for 24 h under a nitrogen atmosphere. After reaction finished, the obtained magnetic nanocatalysts were washed with methanol and dried. The density of catalyst particles was modulated by adjusting the Fe_3O_4 concentration (Table 1).

2.3. Catalyst Characterization. The functional groups of catalysts were determined using a Thermo Fisher Nicolet iS10 FTIR using a KBr tablet. A Netzsch TG 209 F3 Tarsus was used to analyze the thermal stability of Fe_3O_4@PS-CH_2Cl and Fe_3O_4@PS-TMG-n (n = 1−5). The size of catalysts was measured using a Malvern ZS90 DLS. An Elementar Vario MICRO cube elemental analyzer was used to detect the nitrogen content of Fe_3O_4@PS-TMG-n (n = 1−5). The morphology of catalysts was observed using a JEOL JEM-1010 TEM with 80 kV. The static contact angle (CA) between methanol and soybean oil on the surface of catalysts was measured by the Dataphysics OCA-20 sessile drop method. The density of catalysts was measured by the drain away liquid method.

2.4. Preparation and Stability Evaluation of Pickering Emulsions. To obtain Pickering emulsions, Fe_3O_4@PS-TMG was dispersed in anhydrous methanol (2.78 g) with ultrasonication for 2 min. Then, soybean oil (5 g, n(methanol)/n(oil) = 15:1, V(methanol)/V(oil) = 2:3, the same as below) was added to above suspension. The German IKA T18ULTRA-TURRAX high-speed homogenizer was used to emulsify the above system at 10 000 rpm and 25 °C for 60 s. To determine the emulsion type, the obtained emulsions were dripped into the soybean oil phase and methanol phase, respectively. A phase that can disperse the emulsion immediately is the continuous phase (external phase), while the other phase is the dispersed phase (internal phase).[24] Images of the emulsion droplets were taken using an OLYMPUS BX41 optical microscope. The average droplet size of the emulsions was obtained using ImageJ analysis. The volume fraction of emulsion calculated by eq 1 was used to evaluate the stability of Pickering emulsions

$$F = \frac{V_{emulsion}}{V_{total}} \times 100\% \quad (1)$$

where, F is the volume fraction of the emulsion, $V_{emulsion}$ is the volume of the emulsion, and V_{total} is the total volume of the soybean oil/methanol system.

2.5. Biodiesel Production Process under Static Conditions. For biodiesel production via a static transesterification reaction, Fe_3O_4@PS-TMG was dispersed in anhydrous methanol. Then, soybean oil was added (n(methanol)/n(oil) = 15:1). The amount of the catalyst (Fe_3O_4@PS-TMG) was 5.0−10.0 wt % of soybean oil. Then, A high-speed homogenizer (German IKA T18ULTRA-TURRAX) was used to emulsify the above system at 10 000 rpm and 25 °C for 60 s. After stopping emulsification, the emulsion temperature was increased to 60 °C using the circulating heating cooler. In the reaction process, there was no stirring operation. The reaction medium was sampled regularly and a gas chromatograph (GC-2104C, Shimadzu Co., Ltd.) equipped with an Rtx-5 capillary column (length 30 m, i.d. 0.25 mm, film thickness 0.25 μm) and flame ionization detector was used to analyze the content of biodiesel in the sample (temperature program: SPL 240 °C, column 50 °C, SFID 250 °C). After the reaction, the catalyst particles were recovered using magnets, washed with ether and methanol, and dried. The recovered particles were recycled 7 times to determine their activity and stability. Each reaction condition was repeated three times, and the results were averaged.

3. RESULTS AND DISCUSSION

3.1. Synthesis and Characterization of Magnetic Nanocatalysts with Different Densities. Nanospheres consisting of Fe_3O_4 and polystyrene were chosen as the magnetic supporter due to a large density difference between Fe_3O_4 and polystyrene, which provides a facile way to adjust the catalyst density by changing the proportion of each component. Based on the magnetic supporter Fe_3O_4@PS, we first synthesized three magnetic nanocatalysts Fe_3O_4@PS-TMG-n (n = 1−3). FTIR (Figure 1b) and TG measurements (Figure 1c) were carried out to examine the composition of the as-fabricated magnetic nanocatalysts. The characteristic peak of −CH_2Cl (1260 cm^{-1}) almost entirely disappeared in the FTIR spectrum of Fe_3O_4@PS-TMG-n (n = 1−3), while a new band arising from −C═N appeared at 1640 cm^{-1}, indicating that TMG has been successfully loaded on the nanocatalysts. Elemental analysis was also performed to calculate the loading amounts of TMG (Table S1). As shown in Table 1, the TMG loading amounts of Fe_3O_4@PS-TMG-n (n = 1−3) are close to each other, while the density of the catalysts decreases from 1413.3 to 1069.1 kg/m^3. Table 1 also presents the contact angle measurement results, which suggests that Fe_3O_4@PS-TMG-n (n = 1−3) have a similar surface affinity.

In the TG curve of Fe_3O_4@PS-CH_2Cl (Figure S1), a weight loss process can be obviously observed at 180 °C, owing to the

https://doi.org/10.1021/acsomega.1c00629
ACS Omega 2021, 6, 14138−14147

decomposition of $-CH_2Cl$. In comparison, the TG curves of Fe_3O_4@PS-TMG-n (n = 1−3) do not show a steep weight loss at such temperature, which further suggests that $-CH_2Cl$ reacts well with TMG. The residues remaining above 700 °C should be Fe_3O_4 particles. For Fe_3O_4@PS-TMG-n (n = 1−3), the weight proportions of the residues are 34.8, 29.9, and 22.6%, respectively, indicating that the Fe_3O_4 content of the catalyst particle indeed decreases with the reduction of the MNP concentration used for catalyst synthesis.

The particle size of Fe_3O_4@PS-TMG-n (n = 1−3) measured by dynamic light scattering (DLS) is 107, 98, and 82 nm, respectively, and the PDI values lie between 0.14 and 0.23 (Figure S2). Typically, transmission electron microscopy (TEM) images of Fe_3O_4@PS-TMG-3 are shown in Figure 2.

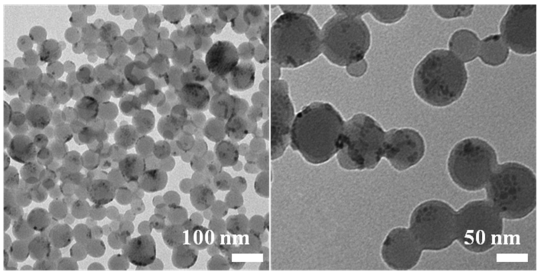

Figure 2. TEM images of Fe_3O_4@PS-TMG-3.

It can be observed that Fe_3O_4@PS-TMG-3 particles contain black internal Fe_3O_4 and shallow outer polymeric shells and exhibit a spherical shape with uniform size. The average particle size of Fe_3O_4@PS-TMG-3 in TEM images is around 80 nm, which is consistent with the DLS measurement results, indicating that the catalyst particles belong to the nanometer category.

3.2. Effect of PIC Density on the Stability of Triglyceride/Methanol Pickering Emulsions. In the presence of Fe_3O_4@PS-TMG-n (n = 1−3) nanoparticles, Pickering emulsions were obtained by stirring the soybean oil/methanol biphasic systems at high speed for 60 s. The dispersion test of the emulsions stabilized by Fe_3O_4@PS-TMG-n (n = 1−3) demonstrated that the internal phase is soybean oil and the continuous phase is methanol.

Appearance and average droplet size of the emulsions placed at room temperature for different times are shown in Figure 3. The initial emulsion volume fractions of all samples are more

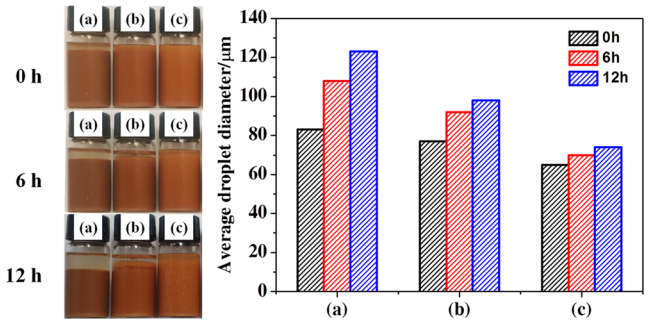

Figure 3. Appearance and average droplet size of soybean oil/methanol (3:2 vol/vol) emulsion stabilized by (a) Fe_3O_4@PS-TMG-1, (b) Fe_3O_4@PS-TMG-2, and (c) Fe_3O_4@PS-TMG-3 at different times under room temperature (25 °C, the amount of catalyst particle is 5.0 wt %).

than 90% (vol/vol). However, over time, the methanol phase obviously appeared on the upper layer of the emulsion stabilized by Fe_3O_4@PS-TMG-1 nanoparticles, and the average droplet diameter drastically increased from 83 to 123 μm, which implies sedimentation and coalescence of the emulsion droplets. A similar phenomenon was also observed in the emulsions stabilized by Fe_3O_4@PS-TMG-2, but the appearance time is relatively late and the change in the oil droplet size is smaller, suggesting that the emulsion suspension stability was improved to some extent. Compared to that of Fe_3O_4@PS-TMG-2, Fe_3O_4@PS-TMG-3 stabilized sample present further improved stability with negligible variation in the emulsion volume and droplet size.

In principle, the destabilization of emulsion originated from the collision and then coalescence of dispersed droplets.[38,40] Under the gravity field, the coalescence of oil droplets might be accelerated by a combined effect of droplet settling and catalyst particle shedding (Figure 4). On the one hand, the sedimentation of oil droplets leads to the generation of a pure methanol phase and a crowded emulsion phase with a higher droplet concentration. In this case, the collision between dispersed droplets is more frequent than that in the initial emulsion. On the other hand, the catalyst particles themselves might come off under the influence of the gravity field, which weakens the protective effects of the catalyst particle layer. To gain more insight into the stability of the soybean oil/methanol Pickering emulsion systems, the detailed process of droplet settling and catalyst particle shedding were analyzed.

In the soybean oil/methanol Pickering emulsion, the oil droplets are affected by gravity G and buoyancy F' (Figure 5a). The resultant force F is given by eq 2

$$F = G - F' = V(\rho_2 - \rho_1)g \tag{2}$$

where ρ_1 is the density of methanol (786.9 kg/m^3), ρ_2 is the density of soybean oil (937.5 kg/m^3), g is the gravitational acceleration, and V is the volume of the droplet. Due to the higher density of soybean oil relative to methanol, the oil droplets tend to settle. In the process of settling movement, the oil droplet will be affected by the friction resistance F_v, which is proportional to the movement velocity: $F_v = fv$, f is the resistance coefficient and v is the settling velocity. When F_v increases to be equal to F, the particles move at a constant velocity,[41] namely

$$fv = V(\rho_2 - \rho_1)g \tag{3}$$

For spherical droplets, it is known from the Stokes formula that $f = 6\pi\eta_1 R$, R is the radius of the droplet and η_1 is the viscosity of the continuous phase. $V = 4\pi R^3/3$, substituting into eq 3, the oil droplet settling velocity is given by eq 4

$$v = \frac{2gR^2(\rho_2 - \rho_1)}{9\eta_1} \tag{4}$$

Here, the viscosity of methanol (η_1) is 0.55 mPa·s (25 °C). The corresponding initial droplet average size D (D = 2R) of Fe_3O_4@PS-TMG-n (n = 1−3) stabilized samples are 83, 77, and 65 μm, respectively, which indicates that as the catalyst particle density and size decreases, the droplet size also decreases. This may be due to the smaller density and size of catalyst particles at the same amount of addition, the corresponding number of catalyst particles being more, thus it is easier to form smaller emulsion droplets for the same

https://doi.org/10.1021/acsomega.1c00629
ACS Omega 2021, 6, 14138−14147

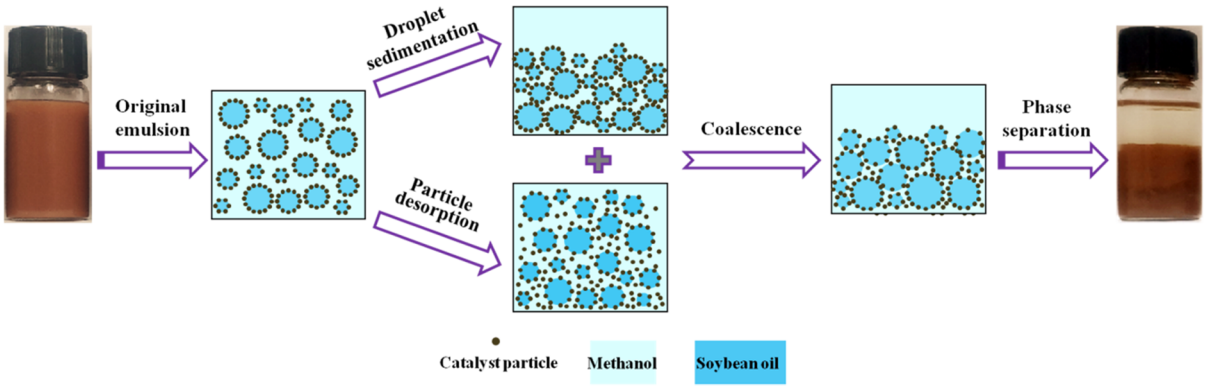

Figure 4. Possible destabilization processes of the soybean oil/methanol Pickering emulsion.

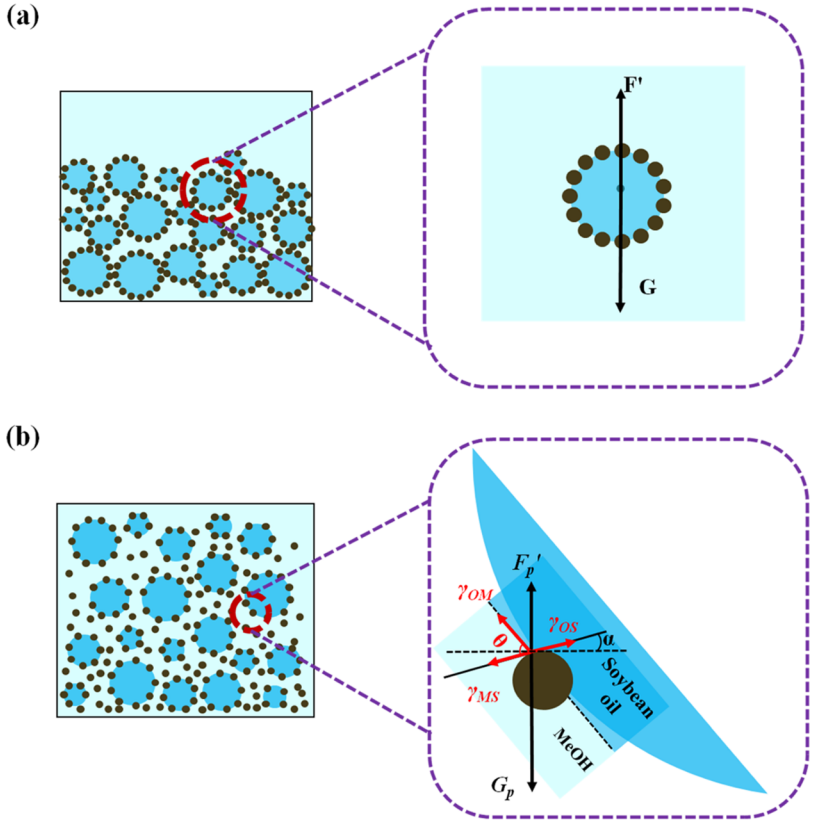

Figure 5. Force analysis of (a) emulsion droplets and (b) PIC particles at the soybean oil−methanol interface.

internal phase volume. According to eq 4, the initial settling velocities of emulsion droplets stabilized by Fe_3O_4@PS-TMG-n (n = 1−3) nanoparticles are 0.1027, 0.0884, and 0.0630 cm/s, respectively. Emulsion droplets stabilized by Fe_3O_4@PS-TMG-1 exhibit the highest settling velocity under the gravity field. In comparison, the emulsion droplets stabilized by Fe_3O_4@PS-TMG-n (n = 2−3) settle relatively slower, which is beneficial for enhancing emulsion suspension stability.

With regard to the PIC particles, they are mainly affected by the gravity G_P, buoyancy $F_{P'}$, and interface adsorption force F_I (Figure 5b). The combined force of gravity and buoyancy (F_P) is calculated by

$$F_P = 4\pi r^3(\rho_S - \rho_1)g/3 \quad (5)$$

where ρ_S is the density of the catalyst particles and ρ_1 is the density of methanol. According to literature research,[42] the energy E required to remove the particle from the interface into the methanol phase is given by

$$E = \pi r^2 \gamma_{OM}(1 - \cos\theta)^2 \quad (6)$$

r is the radius of the adsorbed catalyst particle, γ_{OM} is the oil−methanol interfacial tension, and θ is the three-phase contact angle. The distance (h) required to move the catalyst particle to the methanol phase is given by $h = r\ (1 - \cos\theta)$.[43] Therefore, the interface adsorption force corresponding to the particles is

$$F_I = E/h = \pi r \gamma_{OM}(1 - \cos\theta) \quad (7)$$

It should be noted that the effect of gravity can be passed from one particle to another, causing collective instabilities.[38,44] For simplicity, we evaluated the adsorption stability of the particles at the interface by the ratio of the force of gravitational field to

https://doi.org/10.1021/acsomega.1c00629
ACS Omega 2021, 6, 14138−14147

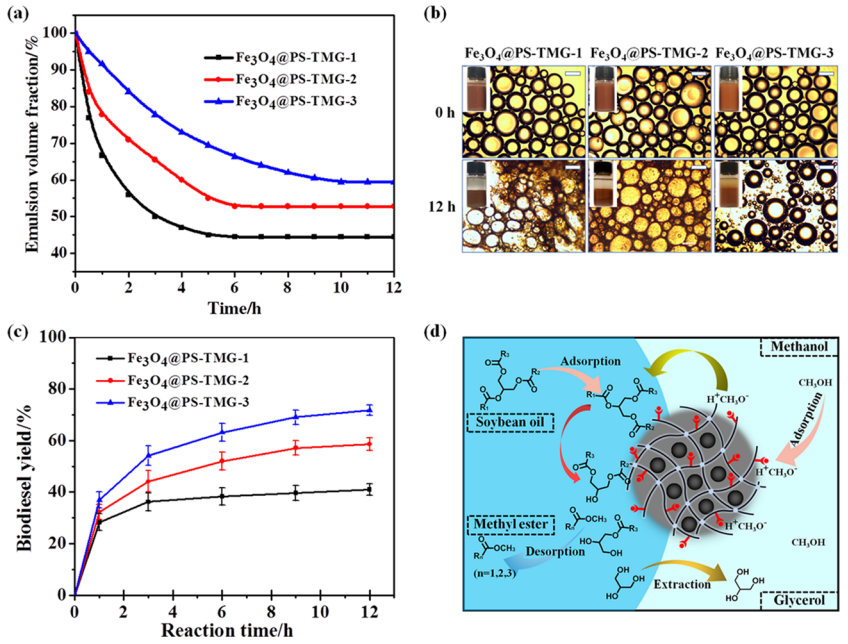

Figure 6. (a) Emulsion volume fraction, (b) appearance and optical microscopy images, and (c) biodiesel yield of soybean oil/methanol (3:2 vol/vol) emulsions stabilized by Fe_3O_4@PS-TMG-n (n = 1−3) at 60 °C (the amount of catalyst particle is 5.0 wt %). (d) The mechanism of transesterification reaction between soybean oil and methanol.

detach particles from the interface to the force of the interface energy to fix the particles at the interface, which is shown in eq 8

$$F_p/F_I = 4r^2(\rho_S - \rho_1)g/3\gamma_{OM}(1 - \cos\theta) \quad (8)$$

Here, parameter B is defined as

$$B = r^2\Delta\rho g/\gamma_{OM}(1 - \cos\theta) \quad (9)$$

where $\Delta\rho$ is the density difference between the catalyst particle and methanol. The contact angles (CA) test (Figure S3) indicates that Fe_3O_4@PS-TMG-n (n = 1−3) exhibit almost the same θ values. Among them, Fe_3O_4@PS-TMG-1 shows the largest B value, mainly due to its higher $\Delta\rho$ value relative to Fe_3O_4@PS-TMG-n (n = 2−3), indicating that Fe_3O_4@PS-TMG-1 particles can be more easily shed from the oil droplet surface under the gravity field. The shedding of catalyst particles increases the coalescence possibility of dispersed droplets, which further increases the droplet settling velocity due to the enlarged droplet size, resulting in rapid emulsion destabilization. In comparison, the B value of Fe_3O_4@PS-TMG-3 with the lowest density is nearly four times lower than that of Fe_3O_4@PS-TMG-1, which is a pivotal factor for its improved adsorption stability.

The analysis of the above two aspects revealed that the main destabilization process of the Pickering emulsion, droplet sedimentation and catalyst particle desorption, can be retarded by reducing the catalyst density. Therefore, Fe_3O_4@PS-TMG-n (n = 2−3) with a lower density relative to Fe_3O_4@PS-TMG-1 exhibit better performance in stabilizing the soybean oil/methanol emulsion.

For transesterification between triglyceride and methanol, an elevated temperature relative to room temperature is usually required to accelerate the reaction. On the basis of previous research, 60 °C is the best optimized temperature for our reaction system.[33] Therefore, we further studied the stability of Pickering emulsions at 60 °C under static conditions (without stirring, except for the initial emulsification stage).

As shown in Figure 6a, in the beginning, the emulsion volume of all samples reduces much faster than that at room temperature. The declined emulsion stability at high temperatures can be ascribed to the following two aspects: (i) the movement and collision of emulsion droplets were enhanced at elevated temperature due to the decreased viscosity of methanol (0.344 mPa·s, 60 °C) and (ii) high temperature exacerbated the Brownian motion of catalyst particles, which made the transfer of gravity from one particle to another more likely to happen, resulting in improved particle shedding probability. Figure 6b shows the appearance and optical microscopy images of the Pickering emulsions at 60 °C. After 12 h, a large amount of opaque solid appeared in the microscopic images of Fe_3O_4@PS-TMG-n (n = 1−2) stabilized samples, indicating the desorption and aggregation of catalyst particles. By contrast, the adsorption of Fe_3O_4@PS-TMG-3 at the soybean oil−methanol interface is demonstrated to be more stable due to its smaller density.

Notably, the declining rate of emulsion volume slows down with time. At 60 °C, the transesterification reaction occurred over time to produce fatty acid methyl ester (biodiesel) and glycerol, accompanied by the generation of intermediate products such as diglyceride and monoglyceride (Figure 6d). The production of fatty acid methyl ester (879.6 kg/m^3) reduced the density of dispersed droplets (ρ_2), while the production of glycerol (1283.0 kg/m^3) with a viscosity of 81.3 mPa·s (60 °C) increased the continuous phase density ρ_1 and viscosity η_1, thereby reducing the droplet settling velocity and particle shedding probability. Besides, the amphipathic intermediate products (diglyceride and monoglyceride) might act as an extra surfactant stabilizer that further improves the emulsion stability.[45] Therefore, as the transesterification reaction proceeds, the emulsion evolves to become more stable, accounting for the lower declining rate of emulsion volume with time.

https://doi.org/10.1021/acsomega.1c00629
ACS Omega 2021, 6, 14138−14147

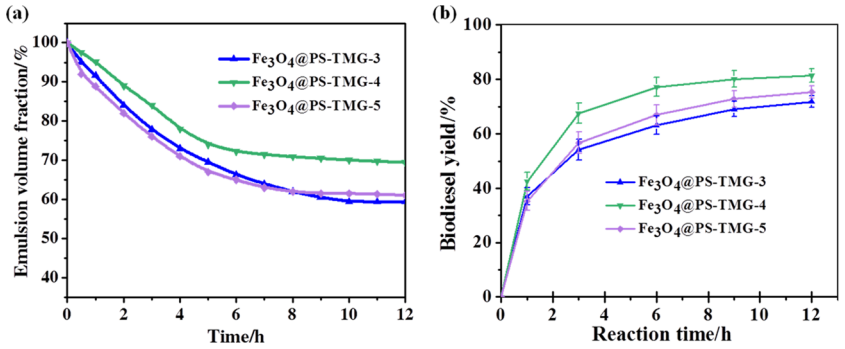

Figure 7. (a) Emulsion volume fraction and (b) biodiesel yield of soybean oil/methanol (3:2 vol/vol) emulsions stabilized by Fe_3O_4@PS-TMG-*n* (*n* = 3−5) at 60 °C (the amount of catalyst particle is 5.0 wt %).

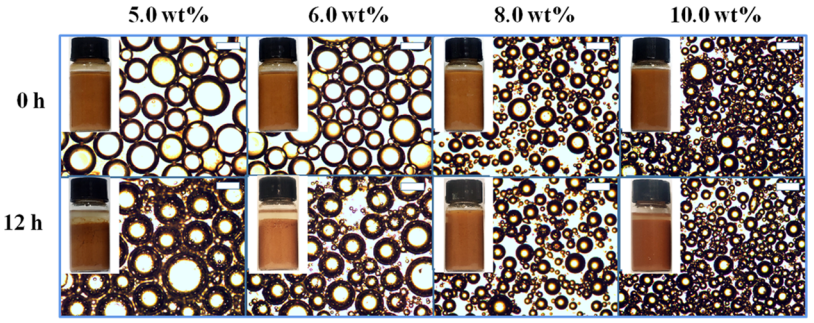

Figure 8. Appearance and optical microscopy images of the soybean oil/methanol (3:2 vol/vol) emulsion stabilized by Fe_3O_4@PS-TMG-4 at 60 °C (the amount of catalyst particle is 5.0, 6.0, 8.0, and 10.0 wt %, respectively, scale is 100 μm).

Figure 6c shows the biodiesel yield of Fe_3O_4@PS-TMG-*n* (*n* = 1−3) stabilized soybean oil/methanol emulsions over time. The emulsions based on Fe_3O_4@PS-TMG-*n* (*n* = 1−2) present lower reaction rates than those based on Fe_3O_4@PS-TMG-3, achieving a biodiesel yield of only 40 and 58%, respectively at 12 h, which can be ascribed to the quickly reduced emulsion stability that leads to insufficient contact with the reactant. By contrast, the emulsion based on Fe_3O_4@PS-TMG-3 showed a relatively higher yield of 71% due to superior emulsion stability that resulted in a larger interfacial area for transesterification. Obviously, improving emulsion stability is vital for improving transesterification efficiency under static conditions. As discussed above, improved transesterification efficiency, in turn, is beneficial for improving emulsion stability.

3.3. Efficient Transesterification under Static Conditions. On account of the favorable performance of Fe_3O_4@PS-TMG-3, we try to finely improve the lipophilicity of the designed magnetic PICs to further enhance the emulsion stability. To achieve this, Fe_3O_4@PS-TMG-4 and Fe_3O_4@PS-TMG-5 were prepared by increasing the molar ratio of St to CMS relative to that of Fe_3O_4@PS-TMG-3 during synthesis. The characterization of Fe_3O_4@PS-TMG-4 and Fe_3O_4@PS-TMG-5 are shown in the Supporting Information (Figures S4−S7 and Table S2). Compared to that of Fe_3O_4@PS-TMG-3, the soybean oil contact angles of Fe_3O_4@PS-TMG-4 and Fe_3O_4@PS-TMG-5 were slightly decreased due to improved lipophilicity. As shown in Figure 7, the emulsion volume and biodiesel yield of Fe_3O_4@PS-TMG-4 stabilized sample are larger than those of Fe_3O_4@PS-TMG-3 stabilized sample during the whole reaction process. Considering that they have almost the same density and particle size (Table 1), the further improved stability should be due to the better lipophilicity of Fe_3O_4@PS-TMG-4 relative to Fe_3O_4@PS-TMG-3, which leads to an increased θ value and consequently a decreased *B* value. However, when the lipophilicity of particles increases further (in the case of Fe_3O_4@PS-TMG-5), the emulsion stability decreased instead. Such a phenomenon can be rationalized by drastically decreasing the maximum capillary force (the pressure that the liquid film formed by the continuous phase can withstand) owing to the over increased θ value that is close to 90°.[46] In this case, coalescence of dispersed droplets becomes easier.

In addition to density and surface affinity, the concentration of catalyst particles also has an important impact on emulsion droplet size and stability under given emulsification conditions.[21] As discussed above, the soybean oil/methanol emulsion stabilized by 5.0 wt % Fe_3O_4@PS-TMG-4 nanoparticles exhibits the best stability and biodiesel yield at 60 °C, but it still exhibits an obvious nonemulsion layer after 6 h. Therefore, we further adjusted the added amount of Fe_3O_4@PS-TMG-4. It can be seen from Figure 8 that when the particle addition amount was increased from 5.0 to 8.0 wt %, the average diameter of the emulsion droplets dramatically decreases from 70 to 39 μm and the emulsion volume remained unchanged in 12 h, showing excellent stability. The enhanced emulsion stability can originate from the following two aspects: (i) with increased particle concentration and decreased droplet size, the surface coverage rate of the droplet is enhanced, which can effectively protect dispersed droplets from coalescence and (ii) the increase of particle concentration increases the viscosity of the continuous phase, thus retarding the motion and collision of dispersed droplets. Nevertheless, when the particle concentration is further increased to 10.0 wt %, the emulsion stability decreases. This is mainly because with the increase of the particle concentration to a certain value, the

https://doi.org/10.1021/acsomega.1c00629
ACS Omega 2021, 6, 14138−14147

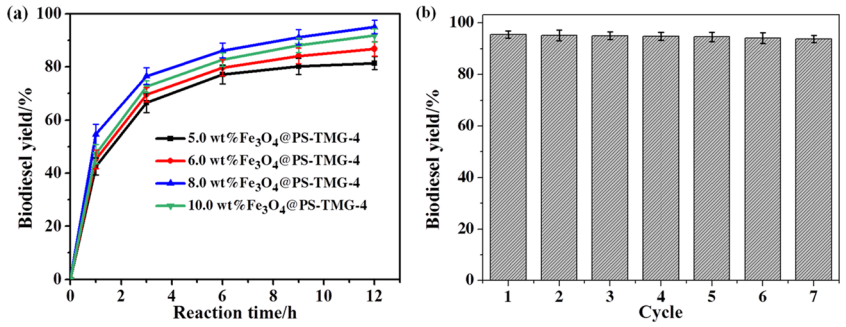

Figure 9. (a) Biodiesel yield of the soybean oil/methanol (3:2 vol/vol) emulsions stabilized by different Fe_3O_4@PS-TMG-4 concentrations under static conditions at 60 °C and (b) recyclability of Fe_3O_4@PS-TMG-4 (8.0 wt %) in the transesterification reaction under static conditions at 60 °C.

droplet diameter remains unchanged, and the excess particles will disperse in the continuous phase or form multi-layer adsorption, which increases the particle collision probability at high temperatures, thus resulting in a greater influence of gravity on the emulsion and a decrease in emulsion stability.

As shown in Figure 9a, with 8.0 wt % Fe_3O_4@PS-TMG-4, the biodiesel yield reached 95.6% after 12 h of static reaction, comparable to our previous work with stirring operation,[33] which suggests that the designed magnetic PIC Fe_3O_4@PS-TMG-4 has great potential for achieving biodiesel production in an energy-saving manner. Besides, compared to other static Pickering systems (Table S3), the optimized reaction system not only represents the highest biodiesel yield with the lowest molar ratio (methanol to oil) but also avoids the use of more complicated autoclave reactors. When the concentration of Fe_3O_4@PS-TMG-4 was increased further, the yield of biodiesel decreased. This should be ascribed to multi-layer adsorption of the particles on the droplets, which hinder the mass transfer at the oil−methanol interface, thereby weakening the reaction intensification effect caused by the enlarged interfacial area.[47] To further embody the catalytic activity of the static transesterification reaction system, we also investigated the catalytic activity of KOH without stirring. Here, the number of active sites is controlled to be equivalent to that of Fe_3O_4@PS-TMG-4 (8.0 wt %). After 12 h, the KOH catalyzed static transesterification reaction system exhibits an extremely low biodiesel yield of only 21.2% due to the large mass transfer resistance (Figure S8).

In addition to high catalytic efficiency under static conditions, the designed magnetic PICs also show significant advantages over KOH, such as recycling capability using a magnet, which significantly simplifies the purification procedure and reduces the generation of waste liquid. After the reaction, Fe_3O_4@PS-TMG-4 was recovered with a magnet and reused for evaluating its catalytic stability. Under the same reaction conditions, the catalytic activity of the recovered Fe_3O_4@PS-TMG-4 only slightly decreased, still retaining a high biodiesel yield of 93.8% at 12 h after 7 cycles (Figure 9b). FTIR analysis and EA results of Fe_3O_4@PS-TMG-4 after being recycled 7 times are shown in Figure S9. The characteristic peak of TMG (1640 cm^{-1}) can be obviously observed and the TMG loading (0.436 mmol/g) remained close to that of the fresh sample, which further demonstrates the stability of the catalyst. The decrease in catalyst activity was mainly due to the existence of a small amount of acid in the raw materials. The high catalytic efficiency and stability of Fe_3O_4@PS-TMG-4 make it a promising catalyst for the green production of biodiesel.

4. CONCLUSIONS

In summary, this work aims at constructing a stable triglyceride/methanol Pickering emulsion via magnetic PIC for achieving efficient transesterification under static conditions. A series of magnetic PICs with a similar TMG loading amount but different densities were first synthesized and utilized as a stabilizer of the soybean oil/methanol emulsion. The variation in the emulsion volume fraction and droplet size revealed that, except for optimizing surface affinity, adjusting the density of PIC particles is also critical to long-time stability of the triglyceride/methanol emulsion (especially at elevated temperatures), owing to the non-negligible effect of gravity on the catalyst particle shedding process. Through adjusting the density of the PIC particles to be close to the density of the continuous phase, finely improving the lipophilicity, and optimizing the addition amount of catalyst particles, we succeed in stabilizing the soybean oil/methanol emulsion for 12 h at 60 °C, which enables efficient transesterification under static conditions, thus resulting in a high biodiesel yield of 95.6% without stirring operation. Moreover, the stability test reveals that the magnetic PIC can be conveniently recycled with a magnet and reused without significant loss of catalytic activity. The static transesterification reaction system offers an alternative strategy for biodiesel production in an environmentally benign and cost-effective way.

■ ASSOCIATED CONTENT

Supporting Information

The Supporting Information is available free of charge at https://pubs.acs.org/doi/10.1021/acsomega.1c00629.

Details about the analytical methods for catalyst density; biodiesel yield and catalyst loading amount; catalyst characterization (TG, DLS, FTIR, and CA); and biodiesel yield using KOH as the catalyst without stirring (PDF)

■ AUTHOR INFORMATION

Corresponding Author

Jianli Wang − *State Key Laboratory Breeding Base of Green Chemistry—Synthesis Technology, Zhejiang Province Key Laboratory of Biofuel, Biodiesel Laboratory of China Petroleum and Chemical Industry Federation, College of Chemical Engineering, Zhejiang University of Technology, Hangzhou 310014, P. R. China;* orcid.org/0000-0002-7525-465X; Email: wangjl@zjut.edu.cn

https://doi.org/10.1021/acsomega.1c00629
ACS Omega 2021, 6, 14138−14147

Authors

Hao Zhang − *State Key Laboratory Breeding Base of Green Chemistry—Synthesis Technology, Zhejiang Province Key Laboratory of Biofuel, Biodiesel Laboratory of China Petroleum and Chemical Industry Federation, College of Chemical Engineering, Zhejiang University of Technology, Hangzhou 310014, P. R. China*

Siyang Yu − *State Key Laboratory Breeding Base of Green Chemistry—Synthesis Technology, Zhejiang Province Key Laboratory of Biofuel, Biodiesel Laboratory of China Petroleum and Chemical Industry Federation, College of Chemical Engineering, Zhejiang University of Technology, Hangzhou 310014, P. R. China*

Shixiong Cao − *State Key Laboratory Breeding Base of Green Chemistry—Synthesis Technology, Zhejiang Province Key Laboratory of Biofuel, Biodiesel Laboratory of China Petroleum and Chemical Industry Federation, College of Chemical Engineering, Zhejiang University of Technology, Hangzhou 310014, P. R. China*

Xiaobo Liu − *State Key Laboratory Breeding Base of Green Chemistry—Synthesis Technology, Zhejiang Province Key Laboratory of Biofuel, Biodiesel Laboratory of China Petroleum and Chemical Industry Federation, College of Chemical Engineering, Zhejiang University of Technology, Hangzhou 310014, P. R. China*

Jun Tang − *State Key Laboratory Breeding Base of Green Chemistry—Synthesis Technology, Zhejiang Province Key Laboratory of Biofuel, Biodiesel Laboratory of China Petroleum and Chemical Industry Federation, College of Chemical Engineering, Zhejiang University of Technology, Hangzhou 310014, P. R. China;* orcid.org/0000-0001-9102-4806

Lingyu Zhu − *State Key Laboratory Breeding Base of Green Chemistry—Synthesis Technology, Zhejiang Province Key Laboratory of Biofuel, Biodiesel Laboratory of China Petroleum and Chemical Industry Federation, College of Chemical Engineering, Zhejiang University of Technology, Hangzhou 310014, P. R. China*

Jianbing Ji − *State Key Laboratory Breeding Base of Green Chemistry—Synthesis Technology, Zhejiang Province Key Laboratory of Biofuel, Biodiesel Laboratory of China Petroleum and Chemical Industry Federation, College of Chemical Engineering, Zhejiang University of Technology, Hangzhou 310014, P. R. China*

Complete contact information is available at: https://pubs.acs.org/10.1021/acsomega.1c00629

Author Contributions

The manuscript was written through contributions from all authors. All authors have given approval to the final version of the manuscript.

Notes

The authors declare no competing financial interest.

■ ACKNOWLEDGMENTS

This work was supported by the Zhejiang Provincial Natural Science Foundation of China (LY18B040004) and the China Postdoctoral Science Foundation (2020M671790).

■ REFERENCES

(1) Lozano, P.; Bernal, J. M.; Sánchez-Gómez, G.; López-López, G.; Vaultier, M. How to Produce Biodiesel Easily Using a Green Biocatalytic Approach in Sponge-Like Ionic Liquids. *Energy Environ. Sci.* **2013**, *6*, 1328−1338.

(2) Gardy, J.; Nourafkan, E.; Osatiashtiani, A.; Lee, A. F.; Wilson, K.; Hassanpour, A.; Lai, X. A Core-Shell SO_4/Mg-Al-Fe_3O_4 Catalyst for Biodiesel Production. *Appl. Catal., B* **2019**, *259*, No. 118093.

(3) Qiu, T.; Guo, X.; Yang, J.; Zhou, L.; Li, L.; Wang, H.; Niu, Y. The Synthesis of Biodiesel from Coconut Oil Using Novel Brønsted Acidic Ionic Liquid as Green Catalyst. *Chem. Eng. J.* **2016**, *296*, 71−78.

(4) Liu, Y.; Lotero, E.; Goodwin, J. G.; Lu, C. Transesterification of Triacetin Using Solid Brønsted Bases. *J. Catal.* **2007**, *246*, 428−433.

(5) Jiang, B.; Wang, Y.; Zhang, L.; Sun, Y.; Yang, H.; Wang, B.; Yang, N. Biodiesel Production via Transesterification of Soybean Oil Catalyzed by Superhydrophobic Porous Poly(ionic liquid) Solid Base. *Energy Fuels* **2017**, *31*, 5203−5214.

(6) Russbueldt, B. M. E.; Hoelderich, W. F. New Rare Earth Oxide Catalysts for the Transesterification of Triglycerides with Methanol Resulting in Biodiesel and Pure Glycerol. *J. Catal.* **2010**, *271*, 290−304.

(7) Leung, D. Y. C.; Wu, X.; Leung, M. K. H. A Review on Biodiesel Production Using Catalyzed Transesterification. *Appl. Energy* **2010**, *87*, 1083−1095.

(8) Feng, L.; Wang, J.; Chen, L.; Lu, M.; Zheng, Z.; Jing, R.; Chen, H.; Shen, X. A Green Strategy to Enhance A Liquid-Liquid Heterogeneous Reaction with A Magnetic Recyclable Pickering Emulsion. *ChemCatChem* **2015**, *7*, 616−624.

(9) de Medeiros, E. F.; Vieira, B. M.; de Pereira, C. M. P.; Nadaleti, W. C.; Quadro, M. S.; Andreazza, R. Production of Biodiesel Using Oil Obtained from Fish Processing Residue by Conventional Methods Assisted by Ultrasonic Waves: Heating and Stirring. *Renewable Energy* **2019**, *143*, 1357−1365.

(10) Maceiras, R.; Alfonsín, V.; Cancela, Á.; Sánchez, Á. Biodiesel Production from Waste Frying Oil by Ultrasound-Assisted Transesterification. *Chem. Eng. Technol.* **2017**, *40*, 1713−1719.

(11) Choedkiatsakul, I.; Ngaosuwan, K.; Assabumrungrat, S.; Mantegna, S.; Cravotto, G. Biodiesel Production in A Novel Continuous Flow Microwave Reactor. *Renewable Energy* **2015**, *83*, 25−29.

(12) Mohod, A. V.; Gogate, P. R.; Viel, G.; Firmino, P.; Giudici, R. Intensification of Biodiesel Production Using Hydrodynamic Cavitation Based on High Speed Homogenizer. *Chem. Eng. J.* **2017**, *316*, 751−757.

(13) Ji, J.; Wang, J.; Li, Y.; Yu, Y.; Xu, Z. Preparation of Biodiesel with The Help of Ultrasonic and Hydrodynamic Cavitation. *Ultrasonics* **2006**, *44*, e411−e414.

(14) Pera-Titus, M.; Leclercq, L.; Clacens, J.-M.; De Campo, F.; Nardello-Rataj, V. Pickering Interfacial Catalysis for Biphasic Systems: From Emulsion Design to Green Reactions. *Angew. Chem., Int. Ed.* **2015**, *54*, 2006−2021.

(15) Zhang, M.; Ettelaie, R.; Yan, T.; Zhang, S.; Cheng, F.; Binks, B. P.; Yang, H. Ionic Liquid Droplet Microreactor for Catalysis Reactions Not at Equilibrium. *J. Am. Chem. Soc.* **2017**, *139*, 17387−17396.

(16) Yang, X.; Wang, Y.; Bai, R.; Ma, H.; Wang, W.; Sun, H.; Dong, Y.; Qu, F.; Tang, Q.; Guo, T.; Binks, B. P.; Meng, T. Pickering Emulsion-Enhanced Interfacial Biocatalysis: Tailored Alginate Microparticles Act as Particulate Emulsifier and Enzyme Carrier. *Green Chem.* **2019**, *21*, 2229−2233.

(17) Jiang, H.; Liu, L.; Li, Y.; Yin, S.; Ngai, T. Inverse Pickering Emulsion Stabilized by Binary Particles with Contrasting Characteristics and Functionality for Interfacial Biocatalysis. *ACS Appl. Mater. Interfaces* **2020**, *12*, 4989−4997.

(18) Crossley, S.; Faria, J.; Shen, M.; Resasco, D. E. Solid Nanoparticles that Catalyze Biofuel Upgrade Reactions at The Water/Oil Interface. *Science* **2010**, *327*, 68−72.

(19) Li, D.; Jiang, J.; Cai, C. Palladium Nanoparticles Anchored on Amphiphilic Janus-Type Cellulose Nanocrystals for Pickering Interfacial Catalysis. *Chem. Commun.* **2020**, *56*, 9396−9399.

(20) Peng, W.; Hao, P.; Luo, J.; Peng, B.; Han, X.; Liu, H. Guanidine-Functionalized Amphiphilic Silica Nanoparticles as A Pickering Interfacial Catalyst for Biodiesel Production. *Ind. Eng. Chem. Res.* **2020**, *59*, 4273−4280.
(21) Zhang, M.; Wei, L.; Chen, H.; Du, Z.; Binks, B. P.; Yang, H. Compartmentalized Droplets for Continuous Flow Liquid-Liquid Interface Catalysis. *J. Am. Chem. Soc.* **2016**, *138*, 10173−10183.
(22) Cho, J.; Cho, J.; Kim, H.; Lim, M.; Jo, H.; Kim, H.; Min, S.; Rhee, H.; Kim, J. W. Janus Colloid Surfactant Catalysts for In Situ Organic Reactions in Pickering Emulsion Microreactors. *Green Chem.* **2018**, *20*, 2840−2844.
(23) Zhang, W.; Fu, L.; Yang, H. Micrometer-Scale Mixing with Pickering Emulsions: Biphasic Reactions without Stirring. *ChemSusChem* **2014**, *7*, 391−396.
(24) Yang, B.; Leclercq, L.; Clacens, J.; Nardello-Rataj, V. Acidic/Amphiphilic Silica Nanoparticles: New Eco-friendly Pickering Interfacial Catalysis for Biodiesel Production. *Green Chem.* **2017**, *19*, 4552−4562.
(25) Zhang, S.; Hong, B.; Fan, Z.; Lu, J.; Xu, Y.; Pera-Titus, M. Aquivion-Carbon Composites with Tunable Amphiphilicity for Pickering Interfacial Catalysis. *ACS Appl. Mater. Interfaces* **2018**, *10*, 26795−26804.
(26) Wei, L.; Zhang, M.; Zhang, X.; Xin, H.; Yang, H. Pickering Emulsion as An Efficient Platform for Enzymatic Reactions without Stirring. *ACS Sustainable Chem. Eng.* **2016**, *4*, 6838−6843.
(27) Dou, S.; Wang, R. The C-Si Janus Nanoparticles with Supported Phosphotungstic Active Component for Pickering Emulsion Desulfurization of Fuel Oil without Stirring. *Chem. Eng. J.* **2019**, *369*, 64−76.
(28) Bago Rodriguez, A. M.; Schober, L.; Hinzmann, A.; Gröger, H.; Binks, B. P. Effect of Particle Wettability and Particle Concentration on the Enzymatic Dehydration of n-Octanaloxime in Pickering Emulsions. *Angew. Chem., Int. Ed.* **2021**, *60*, 1450−1457.
(29) Xue, F.; Zhang, Y.; Zhang, F.; Ren, X.; Yang, H. Tuning the Interfacial Activity of Mesoporous Silicas for Biphasic Interface Catalysis Reactions. *ACS Appl. Mater. Interfaces* **2017**, *9*, 8403−8412.
(30) Zheng, Z.; Wang, J.; Chen, H.; Feng, L.; Jing, R.; Lu, M.; Hu, B.; Ji, J. Magnetic Superhydrophobic Polymer Nanosphere Cage as A Framework for Miceller Catalysis in Biphasic Media. *ChemCatChem* **2014**, *6*, 1626−1634.
(31) Tang, J.; Zhang, Q.; Hu, K.; Zhang, P.; Wang, J. Novel High TEMPO Loading Magneto-polymeric Nanohybrids: An Efficient and Recyclable Pickering Interfacial Catalyst. *J. Catal.* **2017**, *353*, 192−198.
(32) Tang, J.; Zhou, X.; Cao, S.; Zhu, L.; Xi, L.; Wang, J. Pickering Interfacial Catalysts with CO_2 and Magnetic Dual Response for Fast Recovering in Biphasic Reaction. *ACS Appl. Mater. Interfaces* **2019**, *11*, 16156−16163.
(33) Tang, J.; Zhang, Q.; Hu, K.; Cao, S.; Zhang, S.; Wang, J. Novel Organic Base-Immobilized Magneto-polymeric Nanospheres as Efficient Pickering Interfacial Catalyst for Transesterification. *J. Catal.* **2018**, *368*, 190−196.
(34) Macina, A.; de Medeiros, T. V.; Naccache, R. A Carbon Dot-Catalyzed Transesterification Reaction for the Production of Biodiesel. *J. Mater. Chem. A* **2019**, *7*, 23794−23802.
(35) Wang, A.; Sudarsanam, P.; Xu, Y.; Zhang, H.; Li, H.; Yang, S. Functionalized Magnetic Nanosized Materials for Efficient Biodiesel Synthesis via Acid-Base/Enzyme Catalysis. *Green Chem.* **2020**, *22*, 2977−3012.
(36) Bao, Y.; Zhang, Y.; Liu, P.; Ma, J.; Zhang, W.; Liu, C.; Simion, D. Novel Fabrication of Stable Pickering Emulsion and Latex by Hollow Silica Nanoparticles. *J. Colloid Interface Sci.* **2019**, *553*, 83−90.
(37) Melle, S.; Lask, M.; Fuller, G. G. Pickering Emulsions with Controllable Stability. *Langmuir* **2005**, *21*, 2158−2162.
(38) Aveyard, R.; Binks, B. P.; Clint, J. H. Emulsions Stabilised Solely by Colloidal Particles. *Adv. Colloid Interface Sci.* **2003**, *100−102*, 503−546.
(39) Zia, A.; Pentzer, E.; Thickett, S.; Kempe, K. Advances and Opportunities of Oil-in-Oil Emulsions. *ACS Appl. Mater. Interfaces* **2020**, *12*, 38845−38861.
(40) Sacanna, S.; Kegel, W. K.; Philipse, A. P. Thermodynamically Stable Pickering Emulsions. *Phys. Rev. Lett.* **2007**, *98*, No. 158301.
(41) Komaiko, J. S.; McClements, D. J. Formation of Food-Grade Nanoemulsions Using Low-Energy Preparation Methods: A Review of Available Methods. *Compr. Rev. Food Sci. Food Saf.* **2016**, *15*, 331−352.
(42) Fernandez-Rodriguez, M. A.; Binks, B. P.; Rodriguez-Valverde, M. A.; Cabrerizo-Vilchez, M. A.; Hidalgo-Alvarez, R. Particles Adsorbed at Various Non-aqueous Liquid-Liquid Interfaces. *Adv. Colloid Interface Sci.* **2017**, *247*, 208−222.
(43) Binks, B. P.; Lumsdon, S. O. Influence of Particle Wettability on the Type and Stability of Surfactant-Free Emulsions. *Langmuir* **2000**, *16*, 8622−8631.
(44) Tavacoli, J. W.; Katgert, G.; Kim, E. G.; Cates, M. E.; Clegg, P. S. Size Limit for Particle-Stabilized Emulsion Droplets under Gravity. *Phys. Rev. Lett.* **2012**, *108*, No. 268306.
(45) Hu, Z.; Ballinger, S.; Pelton, R.; Cranston, E. D. Surfactant-Enhanced Cellulose Nanocrystal Pickering Emulsions. *J. Colloid Interface Sci.* **2015**, *439*, 139−148.
(46) Kaptay, G. On the Equation of the Maximum Capillary Pressure Induced by Solid Particles to Stabilize Emulsions and Foams and on the Emulsion Stability Diagrams. *Colloids Surf., A* **2006**, *282−283*, 387−401.
(47) Jing, R.; Tang, J.; Zhang, Q.; Chen, L.; Ji, D.; Yu, F.; Lu, M.; Ji, J.; Wang, J. An Insight into the Intensification of Aqueous/Organic Phase Reaction by the Addition of Magnetic Polymer Nanoparticles. *Chem. Eng. J.* **2015**, *280*, 265−274.

https://doi.org/10.1021/acsomega.1c00629
ACS Omega 2021, 6, 14138−14147